Atomic Layer Growth on Al(111) by Ion Bombardment

Carsten Busse,[1] Henri Hansen,[1] Udo Linke,[2] and Thomas Michely[1]
[1]*I. Physikalisches Institut, RWTH Aachen, 52056 Aachen, Germany*
[2]*IGV, Forschungszentrum Jülich, 52425 Jülich, Germany*
(Received 4 January 2000)

Instead of the expected erosion morphology composed of craters, rare gas ion bombardment of the Al(111) surface is found to cause initial surface growth of several atomic layers. This phenomenon is observed for Ne^+, Ar^+, and Xe^+ at all temperatures at which bombardment induces morphological surface changes and for ion energies down to a few hundred eV. The effect is interpreted on the basis of a thermal spike induced separation of damage into subsurface vacancy clusters and surface adatom clusters.

PACS numbers: 61.80.Jh, 68.35.Bs, 68.55.Ln, 81.15.–z

Adatom production due to ion bombardment, predicted by Webb and Harrison in a pioneering molecular dynamics simulation (MDS) [1], has attracted considerable experimental [2–5] and theoretical interest [6–9] in recent years. Under a wide variety of conditions, the adatoms created exceed in number the sputtered atoms [2,6] and can constitute an important part of ion bombardment induced surface damage. The large adatom yields of 10^1–10^2 for keV ion impacts on metals are a consequence of a flow of melt onto the surface, which forms as a result of a thermal spike [3,7]. The resulting damage pattern at low temperatures, where surface diffusion is absent, typically consists of a small crater, several atomic layers deep, surrounded by adatom clusters [10]. Adatom production by energetic particles plays a crucial role in determining the film structure size in ion beam assisted deposition and sputter deposition [4,5] and may be of great importance for the erosive destabilization of a surface under ion bombardment [11].

Despite the importance of adatoms, due to loss of atoms by sputtering, the majority damage species is the vacancy. As a consequence, the characteristic morphology observed after ion bombardment [10,12–15] is dominated by erosion and evolves from surface vacancy islands of monoatomic depth to craters (stacked vacancy islands). As an example of this generic behavior, 1 keV Xe^+ ion bombardment of Pt(111) at 650 K (= 0.32 of the melting temperature T_{melt}) is shown in the insets of Figs. 1(a) and 1(d). We expected a similar erosion morphology for irradiation of Al(111) by 1 keV Xe^+. Our experiments, however, reveal the opposite behavior; namely, at low doses a growth process occurred, which created several new atomic layers before higher doses produced erosion.

The experiments were performed in a variable temperature scanning tunneling microscopy (STM) apparatus [16] with a base pressure of 5×10^{-11} mbar. The Al(111) sample is cleaned by cycles of bombardment with a 1 keV Ar^+ ion beam at 527 K and annealing to 800 K. After preparation, no Auger signals of impurities, including Ar, can be detected, but occasionally the STM pictures exhibited oxide clusters. The average terrace width is about 2000 Å, which made it possible to perform a quantitative analysis only on areas sufficiently far away from preexisting steps. For the irradiation experiments, mass selected ion beams of various ion species and energies at normal incidence with a flux between 8×10^{15} ions/m^2 s and 3.6×10^{16} ions/m^2 s were used. The quantities of removed or created amounts and ion fluences are given in units of monolayer [ML, 1 ML = 1.41×10^{19} (atoms/ions)/m^2 for Al(111)]. STM topographs are shown as differentiated images and appear as if illuminated from the left.

The growth process due to bombardment at 300 K (= 0.32 T_{melt}) can be seen in Fig. 1. Figure 1(a) exhibits adatom islands, but no vacancy islands. The amount of adatoms created evidently exceeds the number of surface vacancies due to sputtering by far. In addition, surface vacancies must be effectively filled with adatoms. In Fig. 1(b) further growth leads to coalescence of the adatom islands and nucleation in the second layer. As ion bombardment proceeds, the first grown layer almost closes, a second layer of adatom islands grows, and a third layer of adatom islands has nucleated [Fig. 1(c)]. In Fig. 1(d) the maximum (1.9 ML) of created material is visible. This exposure marks the transition to the erosion regime since small vacancy islands have nucleated in different layers. This indicates that the flow of adatoms to the surface no longer overcompensates the amount of vacancies created. Further bombardment turns the morphology to the expected erosion one.

An analysis of coverage on the surface is displayed in Fig. 2. In the erosion regime (fluences >0.8 ML), the slope of the coverage versus fluence curve corresponds to the sputtering yield Y. The yields are 4.1 ± 0.4 for 1 keV Xe^+, 2.0 ± 0.2 for Ar^+, and 0.50 ± 0.05 for Ne^+. Material balance requires that adatoms and sputtered atoms be compensated by bulk vacancies. Thus, during the growth phase the amount of bulk vacancies grows and saturates at 4.4 ± 0.4 ML for Xe^+, 1.2 ± 0.1 for Ar^+, and 0.20 ± 0.02 for Ne^+. Once the maximum vacancy concentration below the surface is reached, excess surface vacancies collect to form vacancy islands.

The number and stability of the bulk vacancies are remarkable. For Al bulk irradiation experiments, complete damage annealing is observed at 220 K with the onset of

 0031-9007/00/85(2)/326(4)$15.00

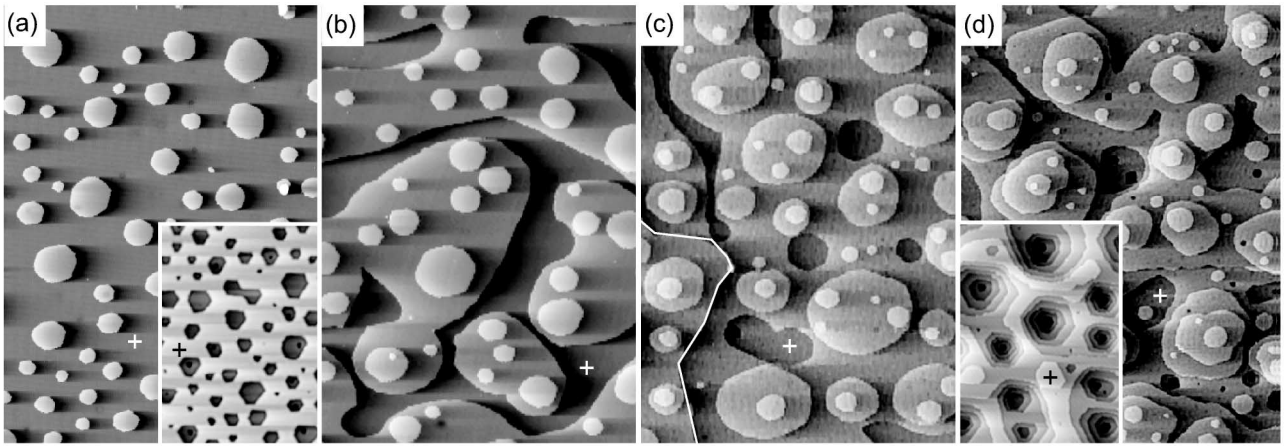

FIG. 1. STM topographs of Al(111) obtained after irradiation at 300 K with 1 keV Xe^+ ion fluences of (a) 0.026 ML, (b) 0.20 ML, (c) 0.34 ML, and (d) 0.51 ML. The amounts grown by bombardment are (a) 0.20 ML, (b) 0.91 ML, (c) 1.4 ML, and (d) 1.9 ML. The initial surface is marked in all topographs by a cross (+). [This qualitative analysis is possible only using additional measurements not shown here, compare Fig. 2 (below).] The topograph sizes are 3300 Å × 2350 Å. The insets (700 Å × 500 Å) show the morphologies after (a) 0.09 ML and (d) 0.7 ML of 1 keV Xe^+ ions on a Pt(111) surface at 650 K resulting in removed amounts of (a) 0.26 ML and (d) 2.1 ML.

vacancy migration (stage III of damage recovery) [17]. Vacancy stabilization by rare gas implantation [18] is not of relevance here, as in the low fluence limit [Fig. 1(a)] at room temperature about 12 stable vacancies remain below the surface after a single 1 keV Xe^+ impact (see below). The nature of the defects becomes evident by annealing experiments [19]. After irradiation with 6×10^{-3} ML 1 keV Xe^+ at 100 K about 0.20 ML of adatoms are created. In an isochronal annealing sequence, the adatom coverage is found to decrease in two distinct steps near 200 to 250 K and near 400 to 450 K. While the temperature of the first annealing step coincides with the onset of vacancy migration, the second annealing step coincides with the onset of vacancy cluster dissociation as determined from annealing sequences following quenching of Al [20]. Thus, we conclude that the vacancies are present as clusters.

Growth by ion bombardment is observed from the lowest investigated temperature of 100 up to 400 K. At higher temperatures the growth turns into erosion by step retraction due to the high mobility of surface defects. The dependence of the effect on the ion species is obvious from Fig. 3 (compare also Fig. 2). The growth effect is strongest for 1 keV Xe^+ bombardment and diminishes for Ar^+ and further yet for Ne^+. As seen in Fig. 3(a), growth is absent for 1 keV He^+ and only small vacancy islands are observed. Growth by ion bombardment is observed at the lowest used energies of 350 eV for Xe^+ and 500 eV for Ar^+. It persists up to the highest investigated ion energies of 8 keV, but the growth effect becomes weaker; e.g., at 300 K and a fluence of 0.025 ML Ar^+ the net created coverages are 0.10 ML for 0.5 keV, 0.13 ML for 1 keV Ar, and 0.07 ML for 8 keV.

A simple model based on MDS of surface damage by energetic particles [7] can explain the observations.

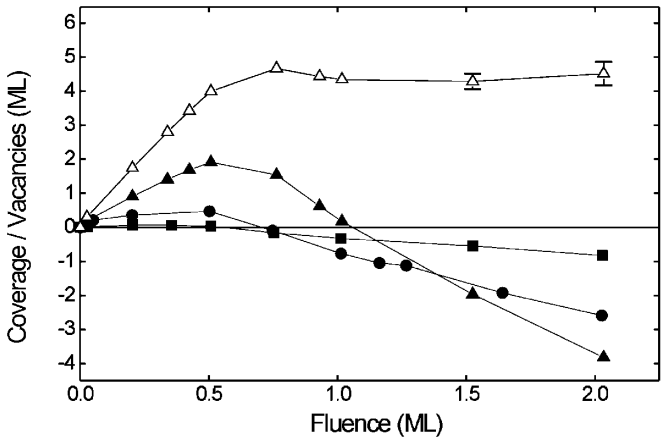

FIG. 2. Evolution of the surface coverage with ion fluence for 1 keV Xe^+ (filled triangles, illustrated in Fig. 1), Ar^+ (circles), and Ne^+ (squares). Positive (negative) values of coverage denote net created (removed) material with respect to the initial surface level. The evolution of bulk vacancies with ion fluence is given for 1 keV Xe^+ (open triangles) only.

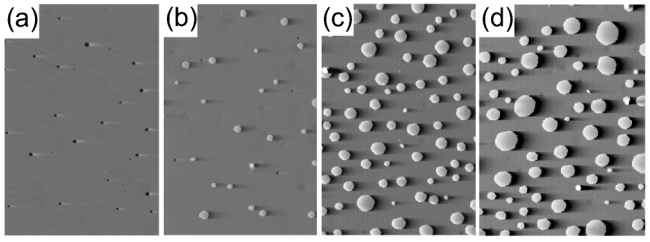

FIG. 3. STM topographs after ion bombardment of Al(111) at 300 K with a fluence of 0.03 ML of 1 keV (a) He^+, (b) Ne^+, (c) Ar^+, and (d) Xe^+ ions. In (a), vacancy islands formed with an area of 0.006 ML, in (b), (c), and (d), adatom islands with areas of 0.02, 0.1, and 0.2 ML, respectively. STM topograph size is 3300 Å × 1650 Å.

Following the collision cascade initiated by the incoming ion, the energy of the moving atoms is distributed uniformly in a small volume; i.e., a thermal spike is formed. A few picoseconds after the initial impact this volume is molten [Fig. 4(a)]. According to MDS of different systems, the melt volume V_{melt} may be estimated by [21]

$$V_{\mathrm{melt}} \approx V_{\mathrm{atom}} \times \frac{E_{\mathrm{nuc}}}{14 k_B T_{\mathrm{melt}}}, \qquad (1)$$

where V_{atom} is the atomic volume, E_{nuc} is the energy available for nuclear collisions [22], and k_B is Boltzmann's constant. The density ρ_{liquid} of liquid Al is lower than the density ρ_{solid} of solid Al at room temperature [23]: $\rho_{\mathrm{solid}}/\rho_{\mathrm{liquid}} = 1.14$. Thus, the liquid droplet formed in the thermal spike is under pressure. If the droplet connects to the surface, the liquid metal can release pressure and flow upward producing adatoms. Recrystallization of the melt proceeds in the bulk from the phase boundary between liquid and solid. The shrinking molten volume decreases in density until finally at least one vacancy cluster in the initial core of the thermal spike is left over [Fig. 4(b)]. The separation of the vacancy cluster from the surface would be especially effective, if the melt was connected to the surface only by a neck, as depicted in Fig. 4. In the case of 1 keV Xe^+/Al, Eq. (1) yields a melt volume of 660 atoms [24]. If the entire excess volume created by melt expansion remains on the surface, one expects $(1 - \rho_{\mathrm{liquid}}/\rho_{\mathrm{solid}}) \times V_{\mathrm{melt}} = 80$ adatoms per impact.

In order to test the model prediction for the adatom yield, we performed experiments at 100 K with very low ion fluences (5×10^{-4} ML) [19]. After 1 keV Xe^+ bombardment single impacts can be distinguished, which produced between one and three closely spaced adatom islands, but no surface vacancies. The measured adatom yield is 50, in surprisingly good agreement with the upper bound value of 80 obtained above.

In view of the outflow model Fig. 1 may be understood as follows: Initially each impact leads to outflow of about 50 adatoms balanced by an equal number of subsurface vacancies. On average about 12 vacancies are created in stable clusters (as can be derived from the initial slope of the coverage vs fluence plot), while the other annihilate with adatoms. The remaining adatoms diffuse and nucleate the large islands seen in Fig. 1. As ion bombardment progresses, the target density decreases to a critical value, at which no more excess volume is created during the phase transition and, hence, no outflow takes place. At this point, the saturation of the surface near layers with vacancy clusters and the maximum grown amount of adatoms are reached. The critical density is to first approximation identical to the density of the liquid. This density can be obtained by distributing the 4.4 ML of vacancy clusters uniformly in a porous zone with a thickness of 30 ML.

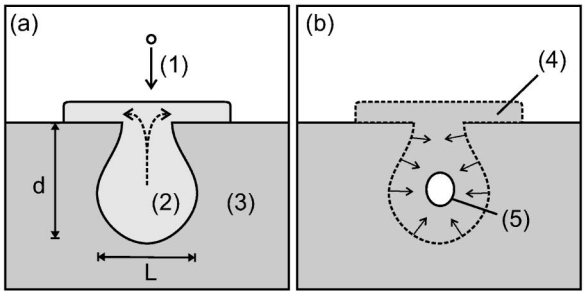

FIG. 4. Schematic sketch of the melt outflow model. (a) As a consequence of the collision cascade initiated by the incoming ion (1), a melt (2) forms below the surface. Material outflow onto the surface occurs as suggested by the dashed arrows. (b) The small arrows show the direction for recrystallization. Adatoms (4) are trapped on the surface and finally a bulk vacancy cluster (5) freezes out.

In the model above, it was assumed that the entire E_{nuc} of the ion contributes to melt formation. However, whether or not a molten volume is formed after the collision cascade and to what extent E_{nuc} is contributing to V_{melt} depends on the energy density deposited. Ions with a high atomic number Z are stopped more efficiently than those with low Z [25] and can transfer their energy to the target in a smaller volume, creating a high energy density. Thus, the amount of outflow decreases in going from Xe^+ to Ne^+ and vanishes for He^+, which exhibits no growth [Fig. 3(a)]. In this case the deposited energy density is not sufficient to induce the phase transition.

The experimentally observed energy dependence of bombardment-induced growth may be related to the depth and shape of the melt volume with the help of the above model. For too low ion energies, the melt formed is shallow with a depth d similar to or less than its diameter L (compare Fig. 4). In this case melt outflow takes place easily, and recrystallization leaves the vacancy rich core connected to the surface. Surface diffusion leads then to the well-known erosion morphology. Bombardment-induced growth becomes efficient, as soon as the melt depth allows to trap the vacancy rich core below the surface during recrystallization, causing bulk vacancy cluster formation. For too high ion energies, the melt volume, although larger, is less connected to the surface and only a small fraction of melt, if at all, flows out. This measured dependence on energy does not correspond to the one proposed in [7], possibly because there the melt volume is modeled by a long cylinder normal to the surface, which is probably not the case here. We note that MDS are highly desirable to clarify the observed behavior. In the case of bulk radiation damage, pressure relief through the outflow of melt is impossible and, consequently, after recrystallization only single vacancies or small vacancy clusters are left behind [26], which anneal completely already at 220 K [17].

Finally, it is necessary to discuss the conditions for reaching the bombardment-induced growth regime. Melt formation, sputtering yield, and ion ranges do not depend at the low ion energies under concern here critically

on crystal orientation. Thus the bombardment-induced growth is most likely a general phenomenon for all Al surfaces including polycrystalline Al. Why was this phenomenon not observed on other metals such as Pt, Au, Ag, and Cu [10–13,15]? We speculate that for Al the optimal melt depth for bombardment-induced growth is reached for impacts with a few hundred eV, i.e., simultaneously with the onset of spike formation. In contrast, for heavier metals the same melt depth is reached only for ion energies above several keV—an energy regime which has not been investigated until now. As an example, binary collision cascade simulations [25] indicate that in order to reach the same ion range as a 350 eV Xe^+ ion in Al, an ion energy above 5 keV is necessary in Pt. In fact, single ion impacts of 4.5 keV Xe^+ on Pt(111) exhibit a crater surrounded by adatom islands, characteristic of a too shallow melt. By increasing the Xe^+ ion energy to 6.5 keV, vacancy cluster formation below the surface could be induced in Pt [27]. Consequently, at this ion energy bombardment-induced growth might take place also on Pt(111).

The phenomenon of bombardment-induced growth is of importance for the growth of Al thin films under the influence of energetic particles, e.g., in ion beam assisted deposition, magnetron sputtering, or ion plating. Thin films of a density close to nominal solid density can be grown only if the cluster dissociation rate exceeds considerably the cluster formation rate. For usual deposition rates of several hundred ML/s, this may be achieved only for deposition temperatures of approximately 300 °C. Below this temperature a porous films structure with low density will result. Implications may be inferior mechanical or electrical properties (e.g., electromigration). The same effect may be relevant for other low Z materials with $\rho_{\text{liquid}} < \rho_{\text{solid}}$, e.g., Be, which is used as wall material in fusion reactors and is exposed to intense irradiation.

In conclusion, we have observed that ion bombardment induces growth of several new atomic layers on a metal surface. This effect is persistent for temperatures, where diffusion of single vacancies is efficient, and vanishes only for temperatures high enough to dissociate vacancy clusters. A model of a flow of melt onto the surface, created by a thermal spike, is able to explain the observations.

The authors acknowledge the help of Matthias Kalff with the Pt(111) experiments, comments by Ralf Detemple, and financial support by the "Deutsche Forschungsgemeinschaft."

[1] R. P. Webb and D. E. Harrison, Jr., Phys. Rev. Lett. **50**, 1478 (1983).
[2] Th. Michely and C. Teichert, Phys. Rev. B **50**, 11 156 (1994).
[3] C. Teichert *et al.*, Phys. Rev. Lett. **72**, 1682 (1994).
[4] S. Esch *et al.*, Appl. Phys. Lett. **67**, 3209 (1995).
[5] M. Kalff *et al.*, Appl. Phys. Lett. **70**, 182 (1997).
[6] H. Gades and H. M. Urbassek, Phys. Rev. B **50**, 11 167 (1994).
[7] M. Ghaly and R. S. Averback, Phys. Rev. Lett. **72**, 364 (1994).
[8] K. Nordlund *et al.*, Nature (London) **398**, 49 (1999).
[9] M. Ghaly, K. Nordlund, and R. S. Averback, Philos. Mag. A **79**, 795 (1999).
[10] Th. Michely and G. Comsa, Surf. Sci. **256**, 217 (1991).
[11] S. Rusponi *et al.*, Phys. Rev. Lett. **81**, 4184 (1998).
[12] J. C. Girard *et al.*, Surf. Sci. **302**, 73 (1994).
[13] M. V. Ramana Murty *et al.*, Phys. Rev. Lett. **80**, 4713 (1998).
[14] S. Jay Chey, J. E. van Nostrand, and D. G. Cahill, Phys. Rev. B **52**, 16 696 (1995).
[15] G. Costantini *et al.*, Surf. Sci. **416**, 245 (1998).
[16] M. Bott, Th. Michely, and G. Comsa, Rev. Sci. Instrum. **66**, 4135 (1995).
[17] P. Erhart, in *Atomic Defects in Metals*, edited by H. Ullmaier, Landolt-Börnstein, New Series, Group III, Vol. 25 (Springer-Verlag, Berlin, 1991), Chap. 2, pp. 88–379.
[18] E. V. Kornelsen and A. A. van Gorkum, J. Nucl. Mater. **92**, 79 (1980).
[19] These experiments will be presented in more detail in a full paper on this topic.
[20] V. Levy, J. M. Lanore, and J. Hillairet, Philos. Mag. **28**, 373 (1973).
[21] W. Schilling and H. Ullmaier, in *Materials, Science, and Technology*, edited by R. W. Cahn, P. Haasen, and K. Kramer (Verlag Chemie, Weilheim, 1993), Vol. 10, Chap. 9, pp. 180–241.
[22] $E_{\text{nuc}} = 0.74$ keV for 1 keV Xe^+/Al as estimated by binary collision cascade simulations [25].
[23] *CRC Handbook of Chemistry and Physics*, edited by D. R. Lide (CRC Press, Boca Raton, 1997).
[24] We note that the estimate of the melt volume on the basis of Eq. (1) is in excellent agreement with MDS for bulk cascades in Al [26].
[25] J. F. Ziegler, J. P. Biersack, and U. Littmark, *The Stopping and Range of Ions in Matter* (Pergamon, New York, 1985).
[26] K. Nordlund *et al.*, Phys. Rev. B **57**, 7556 (1998).
[27] M. Morgenstern and Th. Michely, Philos. Mag. A **79**, 775 (1999).